# ANALYSIS OF MECHANICAL AND THERMAL DISPLACEMENTS OF SPINDLES FOR HIGH-SPEED MACHINE TOOL

**Francisco Augusto Vieira da Silva, francisco.avs@gmail.com**
**Romualdo Figueiredo de Souza, engfsouza@bol.com.br**
**José Carlos de Lima Júnior, limajrcarlos@hotmail.com**
**João Bosco de Aquino Silva, jbosco@ct.ufpb.br**
Universidade Federal da Paraíba, Centro de Tecnologia, Bloco "F" – Campus I – CEP 58.059-900 – João Pessoa – PB, Brasil

**Same format for other authors, if any**

***Abstract.*** Machine tools play a key role in modern industrial production; therefore the technological development of machine tool industry has grown over the past decades. High Speed Machining (HSM) is widely used for machining complex and free form surfaces with high geometrical and dimensional accuracy. The spindle is one of the main items of a machine tool. Thus, it becomes necessary to know the influence levels of the main internal sources of heat in a machine tool. These sources basically derive from: transmission of electric engines; friction in drives and gear boxes; machining process (cutting, chip, workpiece); friction in bearings and guides. The dimensional and geometric accuracy of machined parts depends mainly on the performance of the spindle. To admit the idea of a holistic model, and then propose a possible optimization for a high-accuracy machining it is necessary to study and investigate the mechanical and thermal behaviour of the spindle. For that reason, this paper presents an analysis, based on the finite element method, of the mechanical and thermal deformations, as well as a determination of the critical speed of the spindle of the machine tool at high cutting speed.

***Keywords**: Spindle, Machine Tool, Thermal Deformations*)

## 1. INTRODUCTION (Times New Roman, bold, size 10)

The machine tools are vulnerable to several factors that influence the work part geometric and dimensional quality ranging from: climatic conditions, conditions of the place in which the machining centre is installed, natural environment vibrations, and mainly the internal factors, i.e. the own factors that already come with the machine-tool, such as mechanical and thermal efforts. Regarding the thermal influences, they cause deformations on the structures, therefore, it becomes necessary to know all thermal parameters, for example, the displacements caused by thermal deformation, and temperature distributions, that will affect the spindle turning accuracy, particularly, when it comes to high-quality production. To admit the idea of a holistic model, and then propose a possible optimization for a high-accuracy machining, it is necessary to study and research thermal and structural behavior of machine tools.

To ensure the repeatability in the operation, to manufacture parts with secure dimensional and shape tolerances, and to keep the requirements of surface quality and a high technical performance with economic efficiency have been the requirements that makes us turn directly to the use of machine tools. But to fulfill these requirements, the machine tool must meet some strict project criteria that involve optimal static and dynamic rigidity, thermal stability, easiness operating the machine and an easy access to its internal components, for maintenance purposes.

Currently, the design of machine tools for defined geometry tools machining points to three distinct areas of development. The first is focused in obtaining the maximum flexibility on production and is characterized by hexapod type machines. The second is characterized by the strong action of the removal rate, which forms the basis of high-speed machining – HSM. And the third is focused on meeting the needs to obtain high dimensional and geometric accuracy and surface quality, that is, the ultra precision (Stoeterau, 2004).

Facing the mechanical elements (guides, bearings, spindle, head, etc.) comprising a machine tool, the spindle stands out as one of the main elements. For interfering directly on dimensional and geometric accuracy of the work parts through turning precision, the spindle also conveys the power required for machining.

## 2. Analysis

To determine the displacement curve in defined geometries with constant cross sections and a limited number of boundary conditions, the analytical formulation is feasible, but when the geometry of the structure adopts variable sections (graduated), which is the most common case in this field, the determination of the elastic displacement becomes more complex, and then the finite element analysis method becomes a very powerful tool. The equation governing the dynamic behavior of the elastic line of abeam under bending is given by equation (1) (Silva, 1987a).

$$\rho\ddot{u} + \frac{\partial^2}{\partial s^2}\left(EI\frac{\partial^2 u}{\partial s^2}\right) = w \quad , \quad onde, \ \ddot{u} = \frac{\partial^2 u}{\partial t^2} \tag{1}$$

From the development of Equation (1) results to global finite element equation, expressed by equation (2):

$$\boldsymbol{M_{IJ}\ddot{U}_J + K_{IJ}U_J = F_I} \tag{2}$$

Tal que:
$\boldsymbol{U_J}$ – Displacement Matrix
$\boldsymbol{M_{IJ}}$ - Global Mass Matrix
$\boldsymbol{K_{IJ}}$ - Global Stiffness Matrix
$\boldsymbol{F_I}$ - Force Element Vector

In spread spindles, the analytical analysis are very complex due to the nature of their geometry, but the use of the finite element method makes the analysis practicable for any type of structure. The computational model developed is shown in Fig. (1) and the design parameters are presented below:

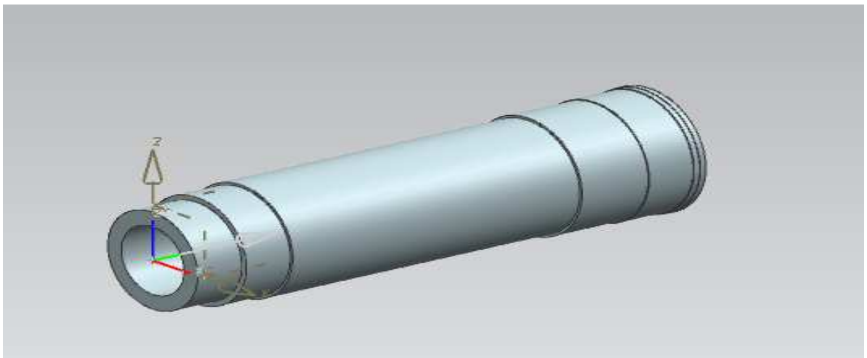

Figure 1. Model developed spindle with multiple cross sections.

The parameters of the analysis in the y direction are: operating force of 1303 N (Node 2), cutting force of 10150 N (Node 8), bending moment of 507300 N.mm (Node 8), modulus of elasticity - 210000 MPa (Steel), rigid bearings located at Node 1 and 5, are applied to beam elements, the discretization of the model is given in items 7 and 8 We and the dimensions of the elements are found in Tab. (1).

Table 1. Dimensions of the elements

| **Element** | **L** (mm) | **De** (mm) | **Di** (mm) |
|---|---|---|---|
| 1 | 40 | 100 | 70 |
| 2 | 40 | 110 | 70 |
| 3 | 260 | 115 | 70 |
| 4 | 60 | 120 | 70 |
| 5 | 40 | 122 | 70 |
| 6 | 5 | 124 | 70 |
| 7 | 5 | 125 | 70 |

The results of displacements and rotations are compared with another computer program that uses the finite element method, the ELFEA2 in Tab. (2) (Silva 1987b):

Table 2. Comparative of displacements and rotations related to the y-axis.

| Node | ELFEA2 ye (µm) | NX yn (µm) | $E_y$ ye-yn (µm) | ELFEA2 θe (rad) | NX θn (rad) | $E_\theta$ θe-θn (rad) |
|---|---|---|---|---|---|---|
| 1 - Node 1 | 0.00 | 0.00 | 0.00 | -0.0000409 | -0.0000355 | -0.0000054 |
| 2 - Node 2 | -1.6 | -1.57 | -0.03 | -0.0000391 | -0.0000341 | -0.0000050 |
| 3 - Node 3 | -3.11 | -3.11 | 0.00 | -0.0000357 | -0.0000307 | -0.0000050 |
| 4 – Node 4 | -3.83 | -3.86 | 0.03 | 0.0000494 | 0.0000542 | -0.0000048 |
| 5 - Node 5 | 0.00 | 0.00 | 0.00 | 0.0000792 | 0.0000839 | -0.0000047 |
| 6 – Node 6 | 3.51 | 4.34 | -0.83 | 0.0000951 | 0.0000999 | -0.0000047 |
| 7 – Node 7 | 3.99 | 4.92 | -0.93 | 0.0000965 | 0.0001012 | -0.0000047 |
| 8 – Node 8 | 4.4 | 5.50 | -1.10 | 0.0000977 | 0.0001024 | -0.0000047 |

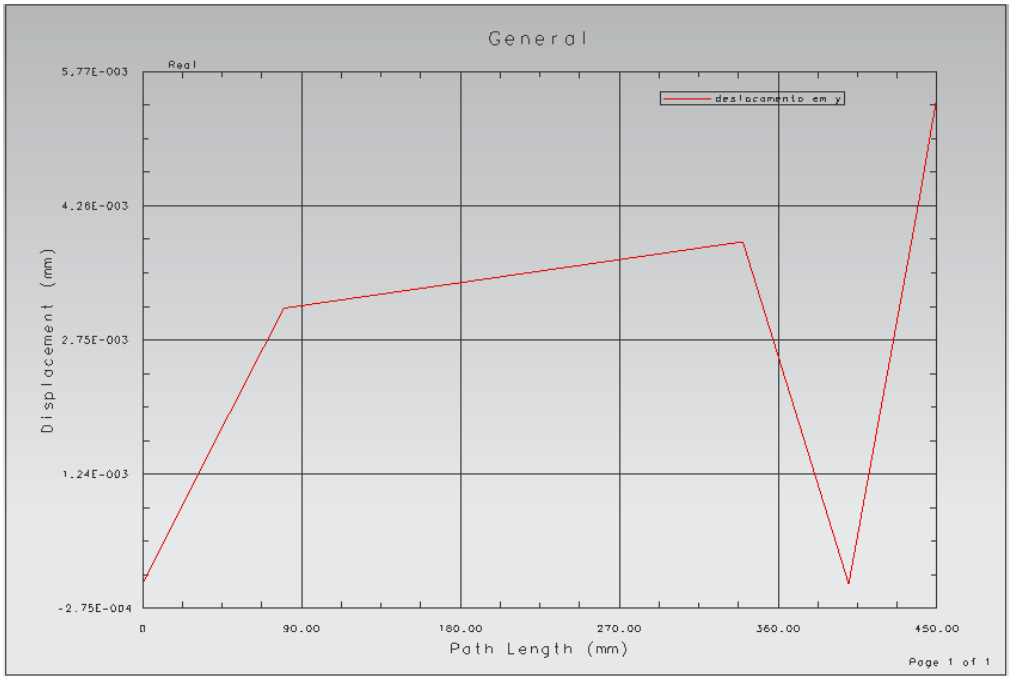


Figure 3. Elastic curve of the spindle in the y direction

The analysis parameters in the x direction are the same used for the calculation of deflection in the y direction, with the exception of efforts where the drive power equals 3581 N, the shear strength of 5073 N and bending moment of 101500 N. mm.

Table 3. Comparative of displacements and rotations related to the x-axis

| Lenght L (mm) | ELFEA2 ye (µm) | NX yn (µm) | Eay ye-yn (µm) | ELFEA2 θe (rad) | NX θn (rad) | $E_\theta$ θe-θn (rad) |
|---|---|---|---|---|---|---|
| 0 - Node 1 | 0 | 0 | 0 | -0.0000031 | -0.0000017 | -0.0000014 |
| 40 - Node 2 | -0.16 | 0.19 | -0.35 | -0.0000055 | -0.0000041 | -0.0000014 |
| 40 - Node 3 | -0.43 | -0.14 | -0.29 | -0.0000077 | -0.0000063 | -0.0000014 |
| 260 - Node 4 | -1.02 | -0.98 | -0.04 | 0.0000122 | 0.0000135 | -0.0000014 |
| 60 - Node 5 | 0 | 0 | 0 | 0.0000223 | 0.0000236 | -0.0000013 |
| 40 - Node 6 | 1 | 1.37 | -0.37 | 0.0000273 | 0.0000286 | -0.0000013 |
| 5 - Node 7 | 1.14 | 1.56 | -0.42 | 0.0000276 | 0.0000289 | -0.0000013 |
| 5 - Node 8 | 1.28 | 1.74 | -0.46 | 0.0000278 | 0.0000292 | -0.0000013 |

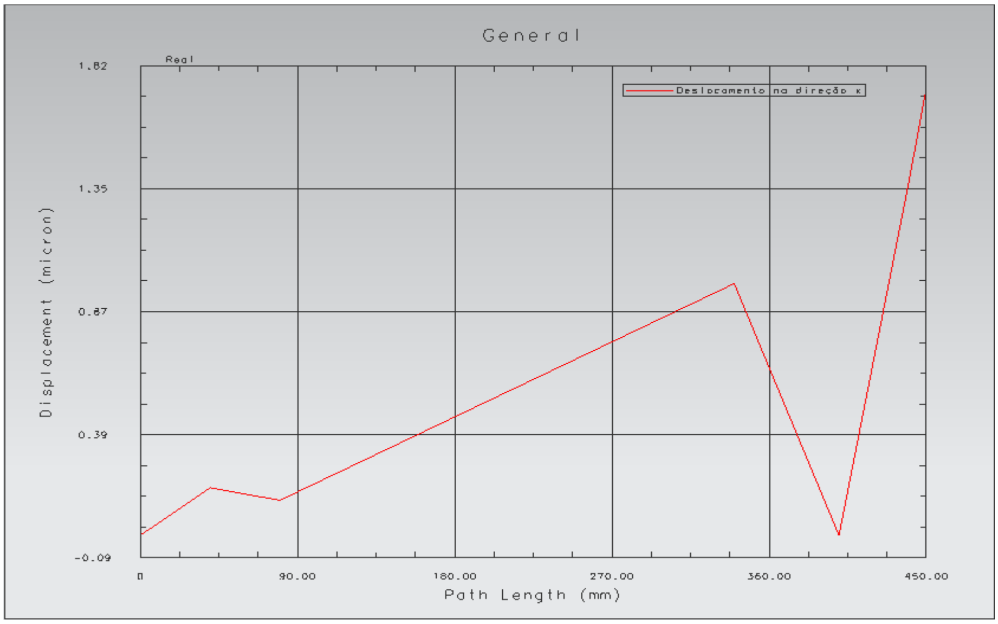


Figure 3. Elastic curve of the spindle in the x direction

Considering the principal stresses within the process of firing and machining, as well as the geometry of the spindle has multiple sections, so the model developed closer examination of the very real. It is observed that higher values of displacement are in the y-axis, which is easily observed by the nature of the machining process, and that the displacement at the tip of the shaft in the y direction is almost three times the amount of displacement in x direction, but this does not minimize in the direction of the deflection less need for compensation of mechanical errors, as the industry's need for accuracy.

### 2.1. Vibration Spindle

As part of calculating the natural frequencies and their respective critical velocities in a spindle without damping and supported by rigid bearings subject to vibration free, it is employing the finite element method. For the case of free vibration from the Eq. (3):

$$M_{IJ}\ddot{U}_J + K_{IJ}U_J = 0 \quad (4)$$

The solution of Eq. (4) is:

$$(|K| - \lambda|M|)\{U\} = 0 \quad (5)$$

Where | K | represents the stiffness matrix, | M | is the mass matrix and $\lambda = \omega^2$; The solution of equation (2) is based on a problem of eigenvalues and eigenvectors. For each eigenvalue there is an eigenvector {λi (U_i}) what is called a natural way. Therefore, the aim of the solution is to determine the pairs of eigenvalues and eigenvectors.

The following data are common to all the free vibration analysis, material is steel, an external diameter of the passage between supports of 100 mm inner diameter stretch between supports of 70 mm, outer diameter of the cantilevered section of 125 mm, inner diameter of the passage in the balance sheet of 87.5 mm, bearings are considered as rigid, is applied to an analysis of the modal type in a spindle discretized into 50 elements and 51 nodes, where beam elements are considered.

Table 4. Results of modal analysis in three spindles of different lengths

| Spindle | Length in balance (mm) | Distance between supports (mm) | Natural Frequencies FRENEA2 / **Nx** (Hz) 1ª | 2ª | 3ª | Critical velocity of the first frequency natural FRENEA2 / **Nx** (rpm) |
|---|---|---|---|---|---|---|
| | | | | | | |
| 1 | 100 | 400 | 1430/**1354** | 4225/**3537** | 8284/**9413** | 85810/**81240** |
| 2 | 400 | 760 | 231/**228** | 878/**640** | 2008/**1798** | 13834/**13740** |
| 3 | 200 | 1.100 | 199/**197** | 706/**687** | 1296/**1201** | 11951/**11820** |

Validated the results found by UGS NX software, which has the largest relative error for the first natural frequency of 5.31%, then it becomes practical and reliable calculation of vibration modes for more complex geometries of spindles, as also in other structures as well as the use for making decisions in designing projects spindles. It is observed that as the length of the spindle increases a significant drop occurs in the natural frequencies - due to the distributed mass is inversely proportional to the angular frequency.

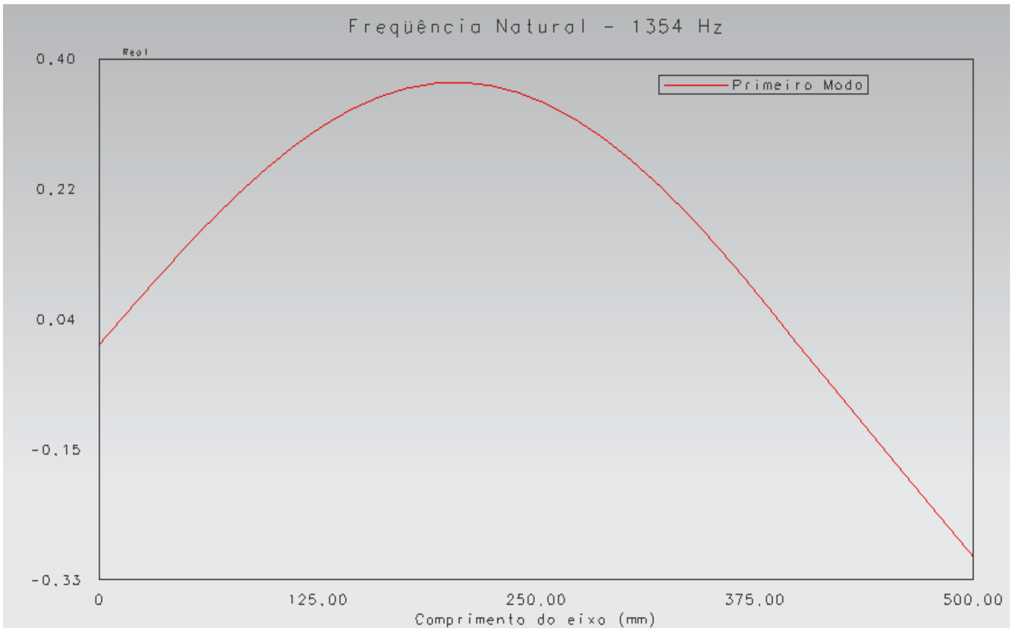

Figure 4. First vibration mode, 1354 Hz

## 2.2. Thermal Analysis

According to Okafor and Ertekin (2000) there are three main sources of errors in machine tools that determine the accuracy of the machine. These are: errors due to geometric inaccuracies, errors, mistakes and thermally induced loads. The direct results of these types of errors are found in the geometric and dimensional errors of part produced. Among these, the thermal errors account for 70% of total errors (HAITAI, 2007).

The errors are generated by changes in ambient temperature, the local sources of heat generated by the sources of activation, the friction in bearings, gears and other transmission devices and the heat generated by cutting process. The errors cause thermal contraction, expansion and deformation of machine tool structure (Silva, 2003a). The spindle is the element that contributes most of the errors in heat, in general, due to the large amount of heat generated from its high speed and heat transferred through the bearings, According to experimental results is the losses in the bearings-the main source of heat, followed by referring to the drive motor. Importantly, the heat generated raises the temperature of the spindle providing thermal strain. These thermal deformations compromise the accuracy of positioning and rotating shaft-bearing system and, consequently, machined parts (Silva, 1987c).

When the problem involves finding the temperature, whose distribution is a function of space and time interpolation function takes the following form (Silva, 2003b).

$$\boldsymbol{T} = \sum_i^n [\boldsymbol{N}]^i \{\boldsymbol{T}\}^i \qquad (6)$$

Where:
***[N]*** $^{i}$ – Matrix of shape functions
***{T}*** $^{i}$ – Nodal temperature

From the equation representing the thermal diffusion and by Gauss' theorem, according to Silva (2003), the heat flux on the boundary are determined. These simulations were performed on two views of analysis. The first point it is the transient thermal analysis and the second case is for the analysis of structural type, where the thermal loads related to temperatures in the boundary conditions and the tip of the spindle, according to the time of collection, are applied to obtain the displacements of the spindle. Figure (5) presents the model developed spindle cross-section and variable cast that features more faithfully the real model. The following parameters are considered as input data for the thermal simulation, distance from the rear bearing and drive gear 50 mm, spindle length between supports of 405 mm (LA), length of the spindle in balance 45 mm (LB), total length of 450 mm (TL = LA + LB), outer diameter of the spindle between supports of 80 mm, inner diameter of the spindle between supports of 50 mm, outer diameter of the shaft-tree swing of 105 mm, inner diameter of the spindle in the balance of 67.5 mm, spindle material is steel, the type of analysis is thermal transient with a duration of 8h, tetrahedral elements are applied with 10 nodes, the model is discretized into a total of 4659 elements and 8837 nodes, the rear bearing temperature is expressed by $T_{md}(t) = 80 - 60e^{-t/900}$, in °C, and the drive gear $T_a(t) = 120 - 100e^{-t/900}$, in °C. The rear bearing and drive gear have higher temperatures, Fig. (6), as a consequence of the rear bearing is designed to withstand higher loads, and temperature of the drive gear is estimated from their condition of work, ie its functionality, its provision on the machine tool to do this, it is your temperature factor equal to one factor used to temperatures of 120 º. The equations applied in the boundary conditions were determined from Newton's law of cooling, where the time constant (τ) the equation was estimated for the boundary conditions are 63% of its final value for the spindle approximately 30 min of operation.

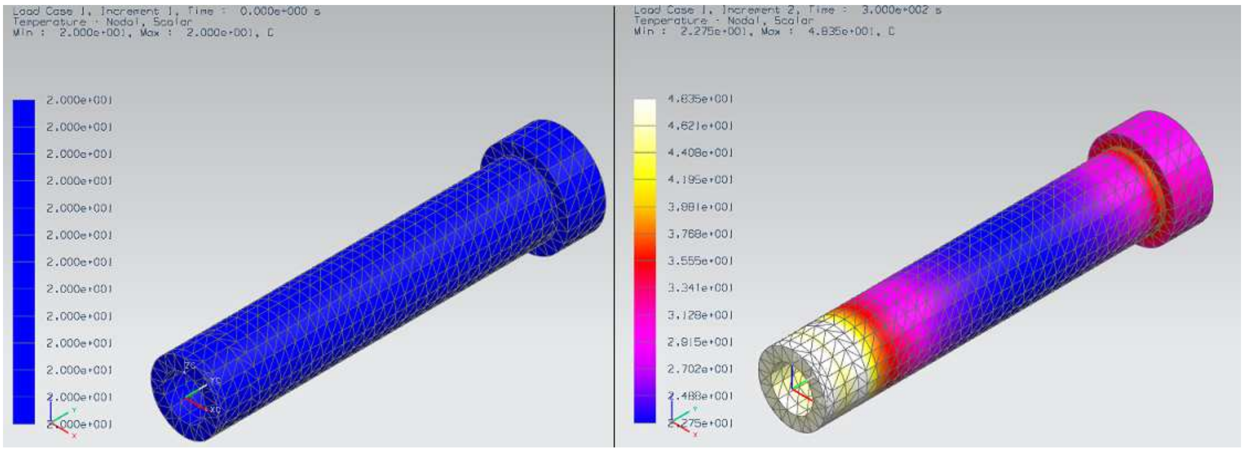


Figure 6. Distribution of temperature starting from the origin to t = 5 min.

The analysis is performed in a time of 8 hours of consecutive operation, in which we provide a collection of data every five minutes, as shown in Fig (7).

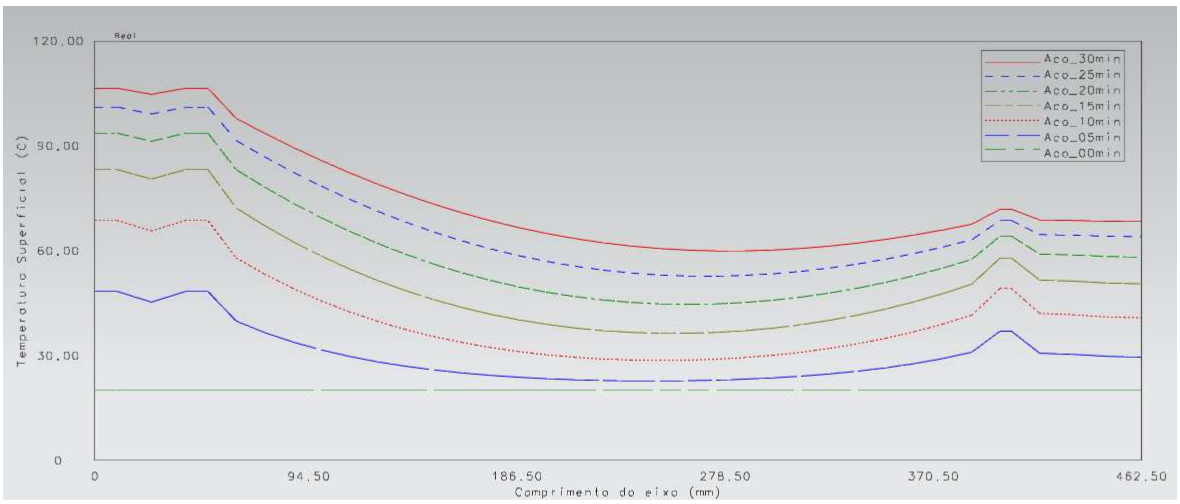


Figure 7. Surface temperatures of the spindle in steel during the first thirty minutes of operation.

In the first thirty minutes of analysis, Fig. (7), we find the temperature rise at all points highlighting the major surface temperatures in the region of the rear bearing and the drive. Note also that, from t = 25 min until t = 30 min heat flux in the spindle is already much smaller compared to the first twenty minutes of analysis, then, from this time interval variations temperature will be minimal.

The Table (5), based on results seen in Fig. (8), becomes noticeable decrease in heat flow over time, so that the growth temperature on the tip of the spindle in the second moment with For the first is 42.6%, while in the third minute against the second is 17.4%, from this trend, we can affirm that the spindle will come into steady state well before the payment of their eight hours of operation. Temperatures collected in Tab. (5) will be applied in the analysis of thermal displacements, so you can draw curves shifts to the spindle at the desired moment.

.

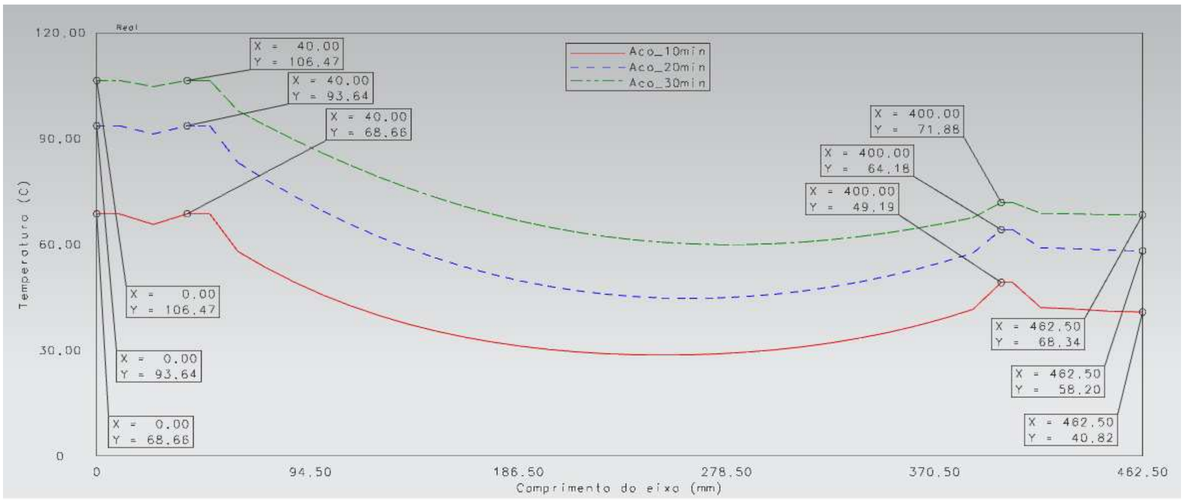


Figure 8. Distribution of surface temperature of steel at t = 10 min, 20 min and 30 min.

Table 5. Surface temperatures of the steel spindle.

| x (mm) | T (°C) | | | |
|---|---|---|---|---|
| | t = 10 min | t = 20 min | t = 30 min | t = 120 min |
| 0 | 68.66 | 93.64 | 106.47 | 120 |
| 40 | 68.66 | 93.64 | 106.47 | 120 |
| 400 | 49.19 | 64.18 | 71.86 | 80 |
| 450 | 40.82 | 58.2 | 68.34 | 80.67 |

For the thermal structural analysis were used the same parameters that are in this section, except for the applied loads and material, where the temperatures were collected on thermal analysis at a given moment, and soon after were subjected to each boundary condition in this spindle, and includes the tip of the spindle, where for the bushing back and drive gear have been temperatures of 120 ° C for the front bearing temperature of 80 º C and the tip of the spindle temperature 80.77 ° C. The simulation performed on a steel spindle can be seen in his state of permanent deformation in Fig. (9).

 

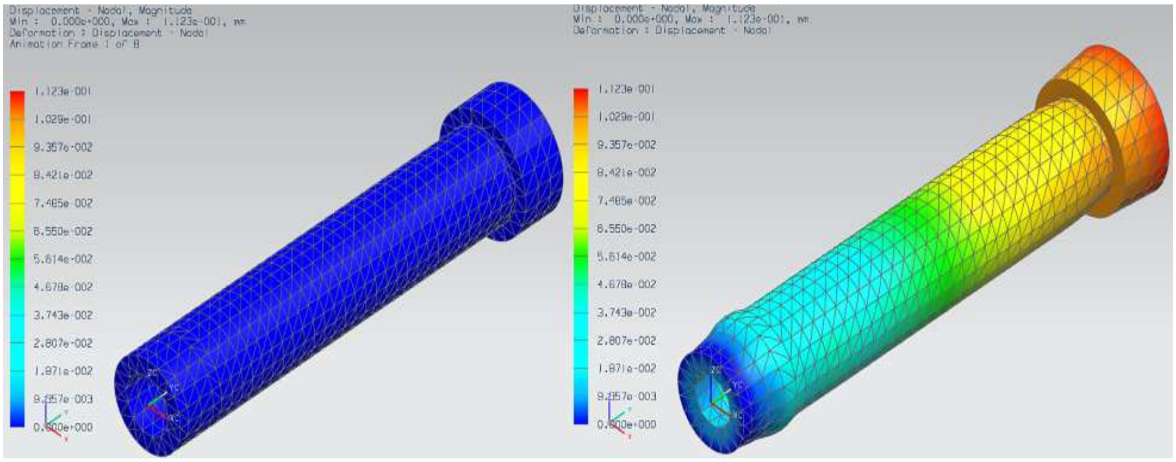


Figure 9. Thermal displacement of spindle subjected to certain temperatures.

Figures (10) to (12) represent the displacements in directions x, y and z, respectively, the spindle steady state. From the analysis it became possible to measure the deformation for each nodal point in time defined by thermal analysis. The importance of determining the deformations in each direction is determined in an optimal position, i.e., position the cutting tool for machining process in such a way that minimizes the errors that would be generated by the advance, but also a compensation for the cutting process.

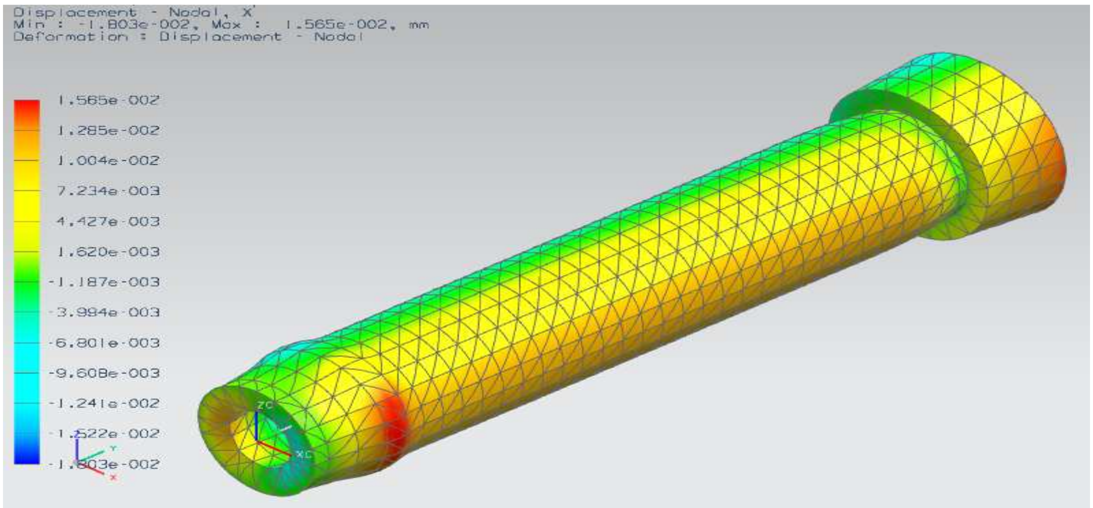


Figure 10. Simulation to determine the displacements in x direction.

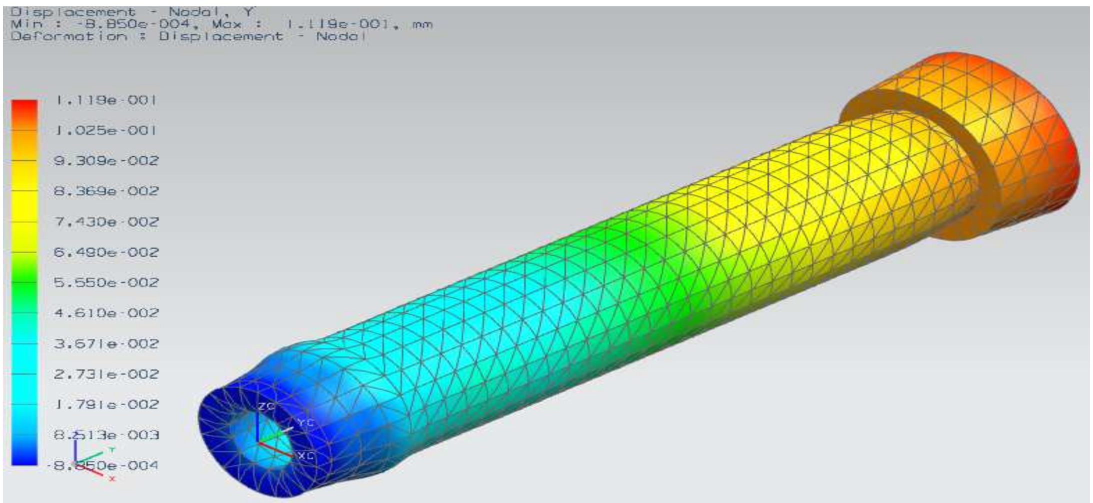


Figure 11. Simulation to determine the displacements in y direction.

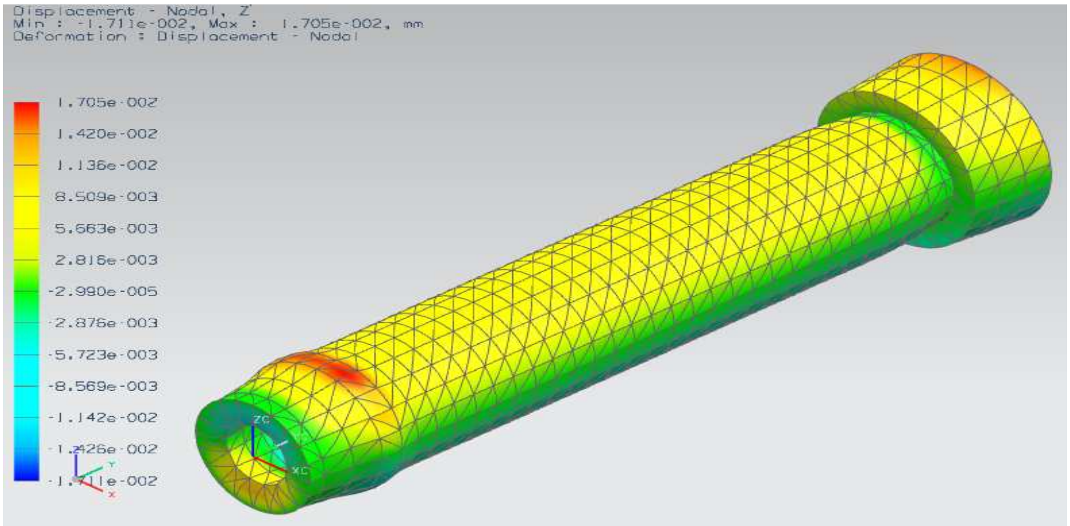


Figure 12. Simulation to determine the displacements in z direction.

It is observed that the largest displacements occur on the upper surface of the spindle in the y direction, same direction as the boundary condition of the front bearing is free. Based on this information, it is determined the offsets for the thirty minutes of initial operation of the spindle in the y direction, Fig. (13).

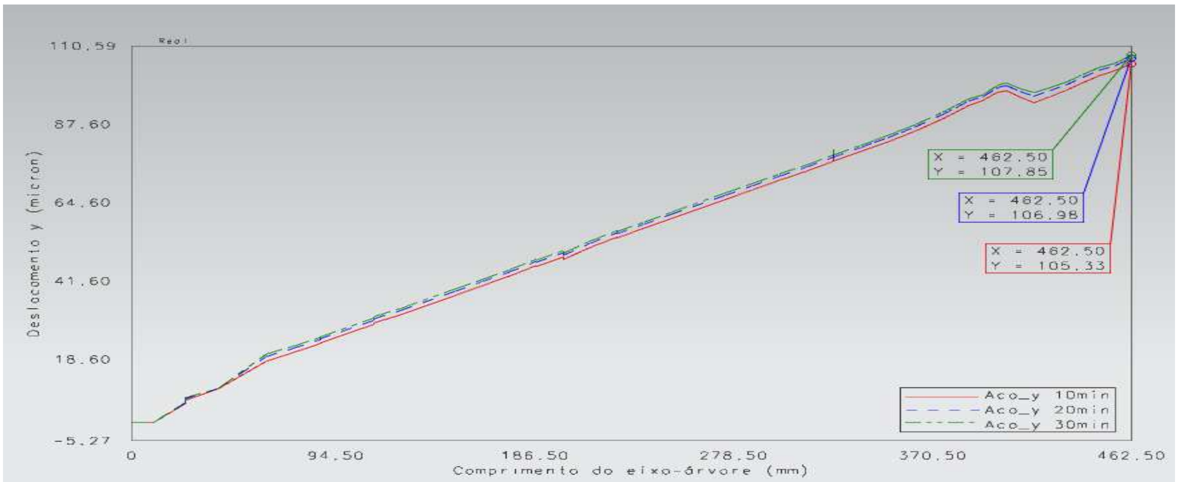


Figure 13. Surface displacement of the spindle in the y direction at t = 10 min, 20 min and 30 min.

In Figure (13) we note a very significant shift from the first line of displacement, t = 10 min. Already in other lines of displacement there is an increase of 1.56% and 0.81% for t = 20 min t = 30 min, respectively. This shows that there is a gradient of displacement that varies over time, and soon, compensatory measures must be taken during the machining process.

**3. CONCLUSION**

The use of finite element method is satisfactory, thus allowing for improvement of future research projects spindles, as well as the minimization of errors caused by geometrical factors discussed and analysis of transient deformations of schemes relating to the operation time of a machine tool.

## 4. REFERENCES

Haitao, et al., 2007, **"Simulation of thermal behavior of a CNC machine tool spindle"**, International Journal of Machine Tools & Manufacture, Vol. 47, pp. 1003–1010.

Okafor, A. C. and Ertekin, Y. M., 2000, **"Derivation of machine tool error models and error compensation procedure for three axes vertical machining center using rigid body kinematics"**, International Journal of Machine Tools & Manufacture, Vol. 40, pp. 1199–1213.

Silva, M. T. Q. S., 2003, **"Análise térmica transiente e de tensões em estruturas executadas em camadas"**, Msc. dissertation, Federal University of Paraná, Curitiba – Paraná, Brazil, 119 p.

Silva, J. B. A., 1987, **"Desenvolvimento do projeto de eixo-árvore de máquinas-ferramenta assistido por computador"**, Msc. dissertation, Federal University of Federal de Santa Catarina, Florianópolis – Santa Catarina, Brazil, 182 p.

Stoeterau, R. L., 2004, **"Introdução ao Projeto de Máquinas-Ferramentas Modernas",** Apostila da disciplina de projeto de máquinas-ferramenta, Curso Engenharia Mecânica, Federal University of Santa Catarina, Santa Catarina, Brazil. 114 p.

## 5. RESPONSIBILITY NOTICE

The author(s) is (are) the only responsible for the printed material included in this paper.